Available online at www.sciencedirect.com
ScienceDirect
Molecular Phylogenetics and Evolution 47 (2008) 523–537
MOLECULAR PHYLOGENETICS AND EVOLUTION
www.elsevier.com/locate/ympev

The first mistletoes: Origins of aerial parasitism in Santalales

Romina Vidal-Russell, Daniel L. Nickrent *

Department of Plant Biology, Southern Illinois University, Carbondale, IL 62901-6509, USA

Received 16 April 2007; revised 11 October 2007; accepted 17 January 2008
Available online 26 January 2008

Abstract

Past molecular phylogenetic work has shown that aerial parasites have evolved five times independently in the sandalwood order (Santalales), but the absolute timing of these diversifications was not addressed. DNA sequences from nuclear SSU and LSU rDNA, and chloroplast *rbcL*, *matK* and *trnL-F* from 39 santalalean taxa were obtained. Separate and combined data partitions were analyzed with maximum parsimony and Bayesian inference. Time estimates were performed with Bayesian relaxed molecular clock and penalized likelihood methods using published fossil data. Both methods gave comparable divergence dates for the major clades. These data confirm five origins of aerial parasitism, first in Misodendraceae ca. 80 Mya and subsequently in Viscaceae (72 Mya), "Eremolepidaceae" (53 Mya), tribe Amphorogyneae in Santalaceae (46 Mya), and Loranthaceae (28 Mya). The rapid adaptive radiation and speciation in Loranthaceae coincides with the appearance of savanna biomes during the Oligocene. In all clades except Misodendraceae, it appears that aerial parasites evolved from ancestors that were polymorphic for either root or stem parasitism—a condition here termed amphiphagous. Convergences in morphological features associated with the mistletoe habit have occurred such as the squamate habit, seed attachment structures, unisexual flowers, and loss of chlorophyll.

Keywords: Misodendraceae; Loranthaceae; Santalaceae; Viscaceae; Eremolepidaceae; Phylogeny; Bayesian relaxed molecular clock

1. Introduction

1.1. Trophic modes in angiosperms

Flowering plants are most often viewed as autotrophs, i.e., photosynthetic organisms that derive their mineral nutrients from water taken up by roots. This stereotypic view ignores the wide diversity of heterotrophic plants that either supplement or replace autotrophism with carnivory, nitrogen fixation, myco-heterotrophism, or parasitism. Parasitic plants establish a direct connection with the xylem or phloem (or both) of their host via modified roots called haustoria. Haustorial parasites are either holoparasites (which do not engage in photosynthesis) or hemiparasites (which do photosynthesize). Current evidence indicates that haustorial parasitism evolved independently in 11 or 12 distinct clades of angiosperms representing ca. 270 genera and over 4500 species (Nickrent, 1997).

Most families of parasitic plants attach to host roots, but others attach to aerial portions of the host. Examples of stem parasites include *Cassytha* (Lauraceae), *Cuscuta* (Convolvulaceae), Apodanthaceae, some species of *Rafflesia*, and mistletoes. Because the term "mistletoe" refers specifically to an aerial parasite that occurs in the sandalwood order (Santalales), it is both taxonomic and a description of plant habit. It has long been accepted that stem parasitic sandalwoods evolved from root parasites (Kuijt, 1969), but there has been disagreement as to the number of times the mistletoe habit evolved. For example, 19th century classification systems placed the mistletoe families Loranthaceae and Viscaceae together, but more recent works (e.g., Barlow, 1964; Wiens and Barlow, 1971) recognized that these families are derived from different ancestors.

* Corresponding author. Fax: +1 6184533441.
E-mail address: nickrent@plant.siu.edu (D.L. Nickrent).

1055-7903/$ - see front matter © 2008 Elsevier Inc. All rights reserved.
doi:10.1016/j.ympev.2008.01.016

1.2. Aerial parasites in Santalales

Santalales includes five clades with aerial parasites (Nickrent, 2002): Misodendraceae, Loranthaceae, "Eremolepidaceae", Santalaceae tribe Amphorogyneae (Stauffer, 1969; Stearn, 1972), and Viscaceae. All Viscaceae, *Misodendrum*, and most Loranthaceae are mistletoes. Previous work (Nickrent et al., 1998; Nickrent and Malécot, 2001) showed that the root parasite *Schoepfia* is not closely related to members of Olacaceae but was sister to *Misodendrum*, an aerial parasite of southern hemisphere beech trees (*Nothofagus*) in Chile and Argentina. This clade is sister to Loranthaceae whose three root parasitic genera are sister to the aerial parasites. It is considered unlikely that the ancestor of this entire clade was a stem parasite and that taxa such as *Nuytsia* and *Schoepfia* "reverted" to the root parasitic condition (Nickrent, 2002). Thus, the phylogeny strongly suggests that the mistletoe habit evolved here twice, once in the ancestor of *Misodendrum* and once in the ancestor of all aerially parasitic Loranthaceae.

In agreement with Wiens and Barlow (1971), the "family" Eremolepidaceae was shown via molecular phylogenetic methods (Nickrent et al., 1998; Nickrent and Malécot, 2001) to be a component of Santalaceae, not sister to Viscaceae (Bhatnagar and Johri, 1983) nor Loranthaceae (Kuijt, 1968). Phylogenetic work using only nuclear 18S rDNA sequences (Nickrent, 2002) showed that a second santalaceous group, tribe Amphorogyneae (*Dendrotrophe* and *Dufrenoya*), was distinct from the eremolepidaceous mistletoes, however, resolution within this group was poor owing to low taxon sampling. All members of Viscaceae are mistletoes and the monophyly of the family is strongly supported (Nickrent et al., 1998; Nickrent and Malécot, 2001). Because this clade emerged from a polytomy involving a paraphyletic Santalaceae, the Angiosperm Phylogeny Group (APG, 1998, 2003) subsumed Viscaceae into Santalaceae. This classification will likely require further revision given that a resolved phylogeny of "Santalaceae" is now available (Der and Nickrent, 2008).

Although it now appears clear that the mistletoe habit arose at least five times independently, the absolute timing of these events has not been addressed. It was suggested (Nickrent, 2002) that *Misodendrum* may represent the first evolutionary "experiment" with the mistletoe habit, but this hypothesis was based solely on the topological position of the *Misodendrum*/*Schoepfia*/Loranthaceae clade between Olacaceae and more derived families where aerial parasitism occurs (Santalaceae, Viscaceae). To properly address this issue, the absolute timings of the five independent events that produced aerial parasites must be directly compared using time-calibrated (ultrametric) trees.

1.3. Timing of diversifications and fossil evidence in Santalales

Within the past decade the botanical community has witnessed the integration of paleobotanical and phylogenetic data, specifically, the calibration of molecular phylogenetic trees with dates derived from fossils. This often provides only minimum ages for nodes because of the possibility of undiscovered older fossils. Moreover, placement of fossils on phylogenetic trees is problematic in that they may be positioned at various points on the stem and crown groups. With good fossil data, transforming relative ages into absolute ages for particular nodes on gene trees would be straightforward if no rate heterogeneity exists (Soltis et al., 2005). Although rate heterogeneity does exist in most groups that have been studied, several methods have been developed that do not rely upon a constant substitution rate (Sanderson, 1997, 2002; Thorne et al., 1998; Huelsenbeck et al., 2000).

Fossils (mainly pollen) of Santalales are well-represented throughout the Cretaceous and Tertiary. One of the major pollen types seen in deposits dating from the Campanian is *Anacolosidites*. This form-genus is extremely variable morphologically, and not all types correspond to Santalales. This was demonstrated in the recent study by Malécot and Lobreau-Callen (2005) who used phenetic methods to discern which palynomorphs were most closely related to modern Olacaceae, tribe Anacolosideae. They concluded that this tribe dated to 70 Mya (Maastrichian) which agrees with broad-based surveys of pollen records for angiosperm orders (Muller, 1984).

Although molecular phylogenetic trees indicate Misodendraceae diverged relatively early in Santalales, fossil pollen records of *Misodendrum* (as *Compositoipollenites*) extend back only to the early Oligocene (Macphail and Cantrill, 2006). In contrast, the form-genus *Aquilapollenites* is known from Maastrichian through Eocene aged strata in a number of locations, although most are from northern hemisphere localities. This pollen type also likely represents more than one phylogenetic group. Jarzen (1977) suggested two lines of development, the isopolar form with a close morphological relationship with Loranthaceae and the second heteropolar to subisopolar form allied with Santalaceae, particularly the genus *Arjona*. Although pollen has been examined for 23 genera of extant Loranthaceae (Feuer and Kuijt, 1979, 1980, 1985; Han et al., 2004), 50 genera remain that have not been studied, thus a comprehensive view of pollen variation across the entire family is lacking. This has confounded attempts to specifically associate form genera such as *Accuratipollis*, *Cranwellia*, *Gothanipollis*, and *Loranthacites* with modern ones (see Couper, 1960; Elsik, 1974; Jarzen, 1978; Menke, 1976; Mildenhall, 1980; Taylor, 1989). Generally the fossil record for Santalaceae is more recent than that of Olacaceae and Loranthaceae. Genera such as *Santalum*, *Osyris*, and *Antidaphne* are known from various Old and New World Eocene deposits (Darrah, 1939; Martin, 1982). Viscaceae records exist from throughout the Tertiary with Eocene records of *Arceuthobium* (Muller, 1981), *Phoradendron* (Darrah, 1939), and *Viscum* (Selmeier, 1975).

1.4. Goals of this study

The objectives of this study are: (1) generate a molecular phylogeny for representatives of Santalales that includes all clades with aerial parasites, (2) utilize Bayesian and likelihood methods, with calibrations obtained from published fossil evidence, to obtain divergence dates for the aerial parasite clades, and (3) compare and contrast the different aerial parasites with respect to ancestral types, timing of divergence, morphological diversity, and convergences.

2. Materials and methods

2.1. Sampling

The ingroup comprises 34 taxa, represented by Viscaceae (three species), Santalaceae including "Eremolepidaceae" (15 species), Opiliaceae (two species), Loranthaceae (10 species), Misodendraceae (two species) and *Schoepfia* (two species). Five species of Olacaceae, *Anacolosa papuana*, *Chaunochitanon kappleri*, *Heisteria concinna*, *Olax emirnensis*, and *Ptychopetalum petiolatum* were used as outgroup for the maximum parsimony (MP) and Bayesian inference (BI) analyses. This sampling represents all families of Santalales and includes all lineages with aerial parasites. Two taxa were missing in each of the nuclear rDNA, *rbcL*, and *matK* alignments, whereas six taxa were missing for the *trnL-F* dataset (see Table 1). Six taxa (mainly Loranthaceae) were missing ca. 600 bp at the 3′ end of the *rbcL* gene. Accession and voucher information for all newly generated sequences (76 total), as well as GenBank numbers all taxa used, are given in Table 1.

2.2. DNA extraction and sequencing

DNA was obtained from silica-dried tissue using a standard CTAB method (Nickrent, 1994). Two nuclear genes, small (SSU rDNA) and large subunit ribosomal DNA (LSU rDNA), were sequenced as were three chloroplast genes: *rbcL*, *matK*, and the *trnL-F* spacer, including the intron between the *trnL* exons. The SSU rDNA was amplified and sequenced using the 12 forward (5′-TCC TGC CAG TAS TCA TAT GC-3′) and 1769 reverse (5′-CAC CTA CGG AAA CCT TGT T-3′) primers. Approximately 950 bp from the 5′ end of the LSU rDNA was amplified and sequenced using the primer pair 27 forward (5′-CCC GCT GAG TTT AAG CAT A-3′) and the 950 reverse (5′-GCT ATC CTG AGG GAA ACT TC-3′). The *rbcL* gene was amplified and sequenced with the 1 forward (5′-ATG TCA CCA CAA ACA GAR AC-3′) and 3′ reverse (5′-TAG TAA AAG ATT GGG CCG AG-3′) or 889 reverse (5′-CTA TCA ATA ACT GCA TGC AT-3′) primers. The gene *matK* was amplified and sequenced with primer 78 forward (5′-CAG GAG TAT ATT TAT GCA CT-3′) and 1420 reverse (5′-TCG AAG TAT ATA CTT TAT TCG-3′). Finally, the *trnL-F* spacer was amplified and sequenced using the primers described in Taberlet et al. (1991).

Standard polymerase chain reactions (PCRs) were used for all genes (Nickrent, 1994). For SSU and LSU rDNA, 5% (final concentration) DMSO was added to the reactions. Cycle sequencing reactions were performed directly on the purified PCR products following standard protocols using BigDye Terminator Cycle Sequencing Ready Reaction Kit with AmpliTaq DNA Polymerase (Applied Biosystems, Foster City, CA) with Better Buffer (The Gel Company, San Francisco, CA). Sequencing reactions were run on an ABI 377 automated DNA sequencer.

2.3. Alignment and phylogenetic analyses

Sequences were aligned by eye in Se–Al (Rambaut, 2004). For *rbcL* and *matK*, inferred amino acid sequences were used to guide the alignment. Ambiguities present in the *trnL-F* intergenetic spacer alignment were discarded from the analysis. MP and BI analyses were conducted on individual genes as well as on a concatenate dataset. MP and bootstrap analyses (100 replicates) were performed with PAUP* v. 4.0b10 (Swofford, 2003). Tree heuristic searches used the Tree Bisection Reconnection branch-swapping algorithm starting with 1000 random addition sequences holding ten trees at each step. Gaps were coded as missing in all analyses.

BI was performed using MrBayes 3.1.2 (Huelsenbeck and Ronquist, 2001; Ronquist and Huelsenbeck, 2003) with a model of molecular evolution chosen via the likelihood ratio test as implemented by MrModeltest (Nylander, 2004). The model selected for each partition was the general time reversible plus a gamma distribution to account for variation among sites and a proportion of invariant sites (GTR+I+Γ). Two independent analyses with four chains each were performed for five million generations, but they were stopped if the average standard deviation of split frequencies between the runs went below 0.01 (reflecting convergence in topology between runs). The relative burn-in used to calculate the standard deviation of split frequencies between the runs was 25%, thus this fraction was deleted from the total number of sampled trees. Trees and parameters were saved every 100 generations. Model parameters were estimated as part of the analysis; uniform prior probabilities were assigned to all parameters except the state frequencies for which a Dirichlet prior distribution was assigned. When more than one partition was analyzed, parameter estimations were unlinked and the rate was set to vary, thus allowing partitions to evolve at different rates.

Character reconstruction (root versus aerial parasite) was performed using parsimony and likelihood in Mesquite (Maddison and Maddison, 2006).

2.4. Molecular dating

Two methods were used to estimate divergence time: Bayesian relaxed molecular clock (BRMC, Thorne et al.,

Table 1
Taxon sampling and GenBank accession information for all sequences used in this study

Name	Collector	DNA Acc. No.	Source	SSU rDNA	LSU rDNA	*rbcL*	*matK*	*trnL-F*
Alepis flavida (Hook. f.) Tiegh.	B. Molloy	2743	New Zealand	L24139	EF464474[b]	N/A	EF464508[b]	EF464481[b]
Anacolosa papuana Schellenberg	R. Regalado and M.Q. Sirikolo 692	4247	Solomon Islands	DQ790104	N/A	DQ790144	EF464516[b]	N/A
Antidaphne viscoidea Poeppig and Endlicher	S. Sargent	2730	Costa Rica	L24080	N/A	L26068	EF464500[b]	N/A
Arceuthobium verticilliflorum Engelm.	D.L. Nickrent and A. Flores	2065	Mexico	L24042	EF464470[b]	L26067	N/A	EF464482[b]
Arjona tuberosa Cav.	J. Puntieri	4131 [s] 4566	Argentina	EF464468[b]	EF464480[b]	EF464532[b]	EF464513[b]	EF464483[b]
Atkinsonia ligustrina (A. Cunn. ex F. Muell.) F. Muell.	D. Watson	4344	Australia	EF464464[b]	EF464475[b]	EF464526[b]	DQ787444	DQ788714
Buckleya distichophylla Torrey	L.J. Musselman	2735	USA	X16598	EF464473[b]	DQ329180	DQ329191	EF464484[b]
Chaunochitanon kappleri (Sagot) Ducke	N. Zamora 1928	3052	Costa Rica	DQ790106	DQ790218	DQ790142	DQ790179	EF464485[b]
Choretrum glomeratum (*F. Muell.*) Benth.	Lepschi and Craven 4602	4312	Australia	EF464461[b]	N/A	N/A	N/A	N/A
Choretrum pauciflorum A. DC.	B. Lepschi, T.R. Lally and B.R. Murray 4237	4222	Australia	N/A	N/A	EF464522[b]	EF464503[b]	N/A
Daenikera corallina Hurlimann and Stauffer	J. Munzinger 2054	4876	New Caledonia	EF464462[b]	EF464472[b]	EF464523[b]	EF464504[b]	N/A
Dendromyza cf. ledermanii (Pilger) Stauffer	D.L. Nickrent T. Kierang, and E. Sape	4466	Papua New Guinea	EF464463[b]	N/A	EF464524[b]	EF464505[b]	DQ340621
Dendrotrophe varians (Blume) Miq.	D.L. Nickrent	2827 [r] 4014 [m]	Australia	L24087	N/A	EF464520[b]	EF464501[b]	DQ340622
Desmaria mutabilis (P. and E.) Jacks.	G. Amico	4510	Chile	EF464465[b]	EF464476[b]	EF464527[b]	EF464509[b]	EF464486[b]
Eubrachion ambiguum (Hooker and Arnott) Engler.	D.L. Nickrent, D. Clark and P. Clark	2699	Puerto Rico	L24141	AF389273	L26071	EF464498[b]	N/A
Gaiadendron punctatum (Ruiz. and Pav.) G. Don.	S. Sargent	2729	Costa Rica	L24143	DQ790209	L26072	DQ787445	DQ788715
Heisteria concinna Standl.	C. Augspurger	2732	Costa Rica	L24146	DQ790230	DQ790161	DQ790197	EF464487[b]
Lepidoceras chilense (Molina) Kuijt.	C. Marticorena and R. Rodríguez 10043	4065	Chile	EF464459[b]	N/A	EF464519[b]	EF464499[b]	N/A
Lepionurus sylvestris Blume	G. Hambali	2879	Java	DQ790101	DQ790206	DQ790131	DQ790170	AF534673
Leptomeria spinosa (Miq.) A. DC.	A. Markey	3081	Australia	EF464460[b]	EF464471[b]	EF464521[b]	EF464502[b]	N/A
Leptomeria aphylla R. Br.	B. Lepschi and A. Whalen 4875	4609	Australia	N/A	N/A	N/A	N/A	EF464488[b]
Ligaria cuneifolia (Ruiz and Pavón) Tiegh.	G. Amico	4567	Chile	L24152	EF464477[b]	EF464528[b]	EF464510[b]	DQ442940
Misodendrum linearifolium DC	D.E. Bran	2829 [s, r][a]	Argentina	L24397	DQ790211	L26074	DQ787438	DQ788712
	G. Amico 136	4591 [l, m, t]						
Misodendrum punctulatum Banks ex DC	G. Amico	3031 [r] 4593	Argentina	N/A	N/A	EF464531[b]	DQ787443	DQ788711
Moquiniella rubra (Spreng. f.) Balle	K. Steiner	3042	South Africa	AF039078	DQ790207	DQ790132	DQ790171	EF464489[b]
Notanthera heterophylla (Ruiz and Pavón) G. Don.	C. Aedo G. Amico	4372 4582 [t]	Chile	EF464466[b]	EF464478[b]	EF464529[b]	EF464511[b]	DQ442939
Nuytsia floribunda (Labill.) R. Br. ex G. Don f.	B. Lamont	2747 3080 [t]	W. Australia	DQ790103	DQ790210	DQ790134	DQ787446	DQ788716
Olax emirnensis Baker	G. Schatz et al. 3620	4035	Madagascar	DQ790119 N/A	DQ790214 N/A	DQ790136 N/A	DQ790173 N/A	N/A AF534674
Opilia amentacea Roxb.	D.L. Nickrent 2816	2816 2809 [t]	Australia	L24407	DQ790202	L26076	AY042621	EF464495[b]
Osyris lanceolata Hochst. and Steud.	Orange Free State Botanic Garden	2731	South Africa	L24409	AF389274	EF464525[b]	EF464506[b]	N/A
Osyris wightiana Wall.				N/A	N/A	N/A	N/A	AY191142

Table 1 (*continued*)

Name	Collector	DNA Acc. No.	Source	SSU rDNA	LSU rDNA	*rbcL*	*matK*	*trnL-F*
Ptychopetalum petiolatum Oliver	E.J. Breteler 14745	4212	Gabon	DQ790121	DQ790215	DQ790138	DQ790175	EF464490[b]
Pyrularia pubera Michx.	L.J. Musselman	2737	USA	L24415	N/A	DQ329179	EF464507[b]	N/A
Pyrularia edulis A. DC.				N/A	N/A	N/A	N/A	AF534679
Quinchamalium chilense Lam.	R. Vidal-Russell	4503	Argentina	EF464469[b]	N/A	EF464533[b]	EF464514[b]	EF464491[b]
Santalum album L.	R. Narayana	2734	India	L24416	AY957453	L26077	AY957453	AY191151
Schoepfia vacciniflora Planchon ex Hemsley.	G. McPherson and P.M. Richardson 15981	3069	Panama	N/A	N/A	N/A	EF464515[b]	N/A
Schoepfia fragrans Wall.	Tsi Zhanhuo 91-417 MO 4252063	5009	China	N/A	N/A	N/A	N/A	DQ788718
Schoepfia schreberi Gmelin	D.L. Nickrent 2599	2599	Bahamas	L24418	AF389261	L11205	DQ787447	DQ788717
Spirogardnera rubescens Stauffer	S. Patrick	4996 5018B [t]	Australia	EF464458[b]	N/A	EF464518[b]	EF464497[b]	EF464492[b]
Tristerix corymbosus (L.) Kuijt	V. Melzheimer	4129 [s, m]	Chile	EF464467[b]	EF464479[b]	EF464530[b]	EF464512[b]	EF464493[b]
	G. Amico	4572 [l]	Chile					
	G. Amico	4597A [t]	Chile					
	G. Amico	4575E [r]	Argentina					
Tupeia antarctica (Forst. f.) Cham. and Schlect.	B. Molloy 2575	2742	New Zealand	L24425	DQ790208	DQ790133	DQ790172	EF464494[b]
Viscum album L.	P. Faber	3024	USA	L24426	AF389275	L26078	N/A	AF180540
Viscum articulatum Burman f.	D.L. Nickrent	2812	Australia	L24427	N/A	EF464517[b]	EF464496[b]	AY191131

[a] Between braces genes for which that accession was used (s, SSU rDNA; l, LSU rDNA; r, *rbcL*; m, *matK*; t, *trnL-F*).
[b] This study.

1998) and penalized likelihood (PL, Sanderson, 2002). To calibrate the Santalales trees, *Saxifraga* was used as outgroup. The root age was set to 114 Mya according to the divergence time estimate of Santalales from Saxifragales determined by a non-parametric rate smoothing analysis of a multigene dataset (SSUrDNA, *rbcL*, and *atpB*) of 560 species of angiosperms (Wikström et al., 2001). To take into consideration the variance of this time estimate, we repeated the analysis setting the root to the lower and upper end of the 95% confidence interval of their estimation i.e., 104 and 124 Mya. Additional Santalales fossils were used as time constraints for crown groups. The first analysis included the outgroup and *Anacolosidites* at 70 Mya (assumed equivalent to extant *Anacolosa* as per Malécot and Lobreau-Callen, 2005). The second analysis included the outgroup, *Anacolosidites*, *Cranwellia* for the crown group of Loranthaceae at 70 Mya (Mildenhall, 1980), *Arjona* at 65 Mya (Chlonova, 1962; Jarzen, 1977), *Santalum* at 65 Mya (Darrah, 1939; Christopher, 1979) and *Arceuthobium* (as *Spinulaepollis arceuthobioides*) at 52 Mya (Krutzsch, 1962).

The BRMC method was implemented utilizing the software MULTIDIVTIME (Thorne et al., 1998). This method approximates the mean posterior probabilities of substitution rates and divergence times with credibility intervals obtained through the Markov Chain Monte Carlo algorithm. The protocol from the manual by Rutschmann (2005) as well as the Readme files from the program were followed. The topology used for the analysis was the one obtained with BI using the five genes, but only *matK* and *rbcL* were used for estimating divergence time. These two genes were chosen because they had the most complete sampling, are derived from one linkage group (the chloroplast genome), and have similar rates of evolution.

Parameters estimated with BASEML (Yang, 1997) under the F84 model were used to estimate branch lengths and the variance–covariance matrix in ESTBRANCHES. The output file from this program was used as input for MULTIDIVTIME. The Markov chain was run for 1 million generations sampling every 100 generations. The burn-in was set to be 10% of the samples (1000 trees). We used 1.14, 1.04 and 1.24 (114, 104 and 124 Mya, respectively) for the expected number of time units between tip and root with standard errors of 0.57, 0.50 and 0.62, respectively. The prior for the rate was obtained by dividing the median of the branches by the time from the ingroup root to the tips, resulting in 0.1 substitutions/site/time unit. The Brownian motion parameter (nu) that controls the degree of rate autocorrelation along the descending branches of the tree was set so that the time units from root to tip multiplied by nu was approximately 1.0, as recommended in the manual. A total of 10 runs with the same settings, but different seeds, were performed to check for consistency in the results.

The PL method was implemented with r8s software (Sanderson, 2003). This approach allows each branch to have its own average rate, invoking a penalty function that controls rate variation over time. Branch lengths used to

estimate node ages were obtained using maximum likelihood in PAUP* under the GTR+I+Γ model of sequence evolution. The smoothing parameter was estimated via cross-validation. The tree root date was set to 114, 104 and 124 Mya and the dates for the santalalean fossil lineages (above) were used as time constraints.

3. Results

3.1. Variability of the nuclear and chloroplast markers

The nuclear SSU rDNA matrix consisted of 1832 aligned sites of which 175 were parsimony informative. Thirty-two most parsimonious trees were found, each 720 steps in length. The nuclear LSU rDNA dataset consisted of 972 aligned sites of which 177 were parsimony informative. Four equally parsimonious trees were found of length 891 steps. Because the SSU and LSU rDNA matrices, when analyzed separately, resolved very few clades, they were concatenated. This is justified given these regions occur within the same transcriptional cistron. In this analysis, 51 most parsimonious trees were found of 1705 steps. The chloroplast gene, *rbcL*, had 1437 aligned positions of which 267 were parsimony informative. The second chloroplast gene *matK* had 1387 aligned positions of which 554 were parsimony informative. Parsimony analysis yielded nine trees of length 2379. The *trnL-F* region consisted of 862 aligned sites of which 210 were parsimony informative (after exclusion of ambiguous sites mainly from the spacer between the *trnL* and *trnF* genes). The search of the *trnL-F* region matrix resulted in 4680 trees of 761 steps.

3.2. Topologies of the separate gene trees

Tree topologies resulting from analyses of the combined SSU and LSU rDNA and the individual chloroplast genes are shown in Fig. 1. For the rDNA data (Fig. 1A), a monophyletic Loranthaceae was supported (BS = 73, PP = 1.0) which was sister to a clade composed of Misodendraceae, *Schoepfia* and *Arjona* (BS = 88, PP = 1.0). Two other major clades were recovered by this analysis, one corresponding to Opiliaceae (BS = 100, PP = 1.00) and another to Santalaceae (BS = 66, PP = 0.93) including a monophyletic Viscaceae. The relationship between these three main clades was not well supported. Compared with the rDNA tree, the *rbcL* partition resolved additional clades (Fig. 1B). Strong support (BS = 84, PP = 1.0) was obtained for the clade composed of a monophyletic Loranthaceae and its sister clade Misodendraceae plus *Schoepfia*, *Arjona* and *Quinchamalium*. Support for some clades within Santalaceae was obtained, e.g., the eremolepidaceous mistletoes (PP = 0.92), Amphorogyneae (BS = 80, PP = 1.0), and Viscaceae (BS = 100, PP = 1.0), but relationships among the major clades were not strongly supported. The chloroplast gene *matK* (Fig. 1C) recovered two major clades, one composed of Loranthaceae, Misodendraceae, *Schoepfia*, *Arjona* and *Quinchamalium* (BS = 69, PP = 1.0) and another that included Opiliaceae, Santalaceae and Viscaceae (BS = 73, PP = 1.0). Strong support was obtained for Misodendraceae, Loranthaceae, Opiliaceae, and two clades within Santalaceae, but relationships among these families was poorly supported. The *trnL-F* region (Fig. 1D) recovered the same two major sister clades obtained with *matK*. The first included Loranthaceae, Misodendraceae, *Schoepfia*, *Arjona*, and *Quinchamalium* (BS = 79, PP = 1.0). Within the first clade, Misodendraceae was sister to a clade formed by *Schoepfia*, *Arjona*, and *Quinchamalium* (BS = 76, PP = 0.65), and Loranthaceae was monophyletic (BS = 86, PP = 1.0). The other major clade comprised Opiliaceae, Viscaceae and the remaining genera of Santalaceae (BS = 78, PP = 1.0). Although, Opiliaceae and Viscaceae were monophyletic with high support, the relationship among these three families was not resolved.

3.3. Topology of the concatenated data tree

Trees from the four separate data partitions (Fig. 1A–D) differed mainly in their levels of support for various clades; no strong support was obtained for conflicting clades. For this reason, data from all partitions were concatenated. This matrix had 6490 aligned positions of which 1415 were parsimony informative. MP analysis yielded three most parsimonious trees of 6080 steps. The three tree topologies differed only in relationships among genera of aerially parasitic Loranthaceae. Relationships among the major santalalean clades were completely resolved and each node received high bootstrap support in MP as well as high BI posterior probabilities. The majority rule BI consensus tree (Fig. 2) will thus be used to infer the origin of aerial parasitism in the order.

The BI consensus tree is composed of two major sister clades, each of which contains root and aerial parasites (clades of interest labeled A–H in Fig. 2). The first major clade contains a monophyletic Loranthaceae (clade C) which is sister to another composed of Misodendraceae (clade A) and clade B that contains *Schoepfia*, *Quinchamalium* and *Arjona*. Within clade B the two species of *Schoepfia* are sister to *Arjona* and this clade is sister to *Quinchamalium*. For Loranthaceae, the western Australian root parasitic tree *Nuytsia* is sister to the remaining members of the family. The next two diverging taxa, *Gaiadendron* (New World tropics) and *Atkinsonia* (eastern Australia), are also root parasites. *Atkinsonia* is weakly supported as sister to the remaining seven genera, which are all aerial parasites. Relationships among the aerial parasite clades received low MP bootstrap support.

The second major clade (D–H) contains representatives of Opiliaceae, Santalaceae and Viscaceae. Here the two root parasitic genera of Opiliaceae are monophyletic (clade D) and are sister to the remaining clades E–H. Clade E is composed of the root parasites *Pyrularia* and *Buckleya*. Clade F contains five genera, two of which are root parasites (*Osyris* and *Santalum*) and the remaining three are

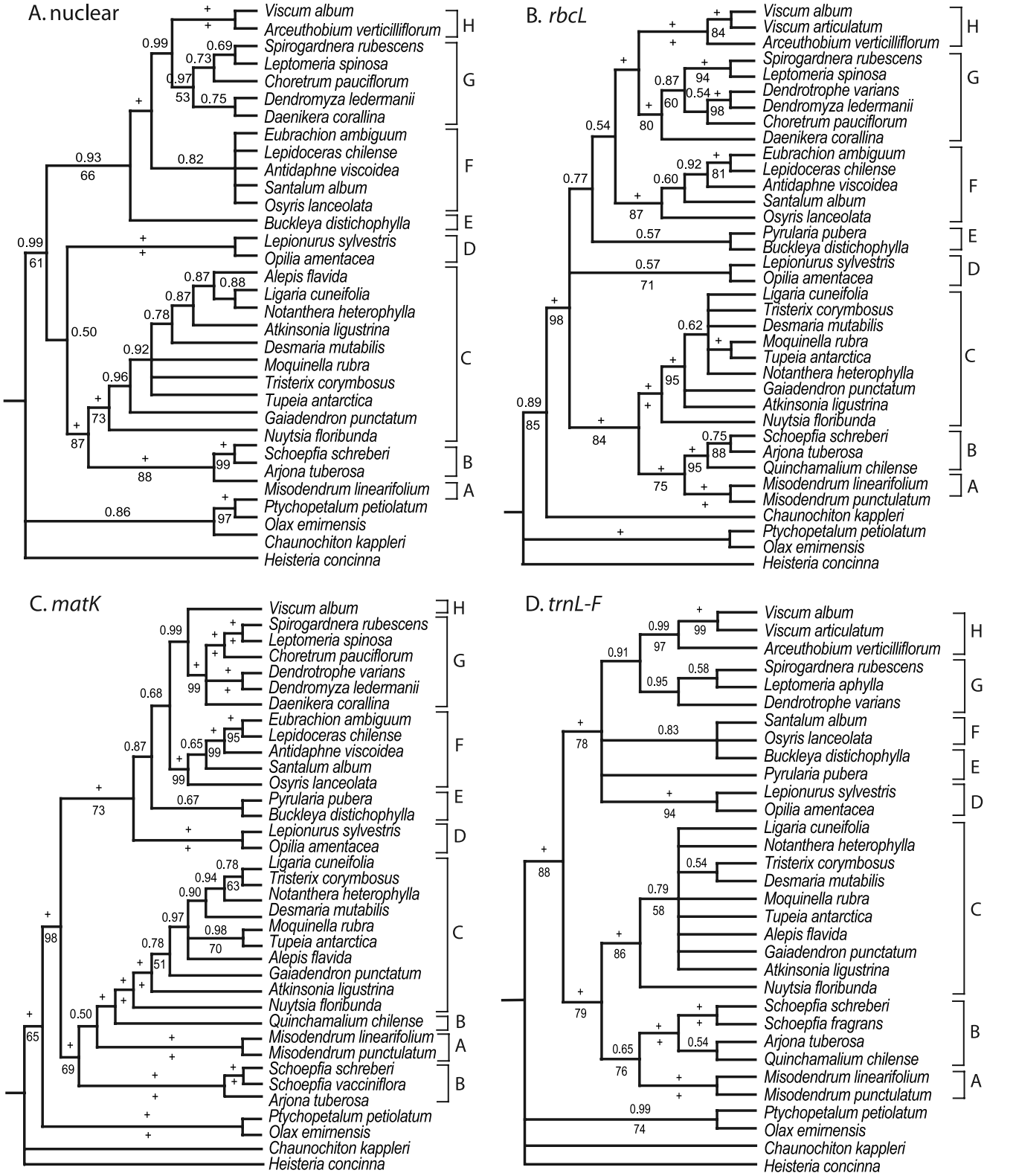

Fig. 1. Gene trees derived from Bayesian analyses of the different partitions. The nuclear SSU and LSU rDNA matrices were concatenated and analyzed together.

New World mistletoes previously classified in their own family Eremolepidaceae. Clade G, representing tribe Amphorogyneae, is composed of root and stem parasites as well as a dendroparasite (*Dendrotrophe*—see Section 4). Clade H contains two long-branch taxa that are typically classified in Viscaceae.

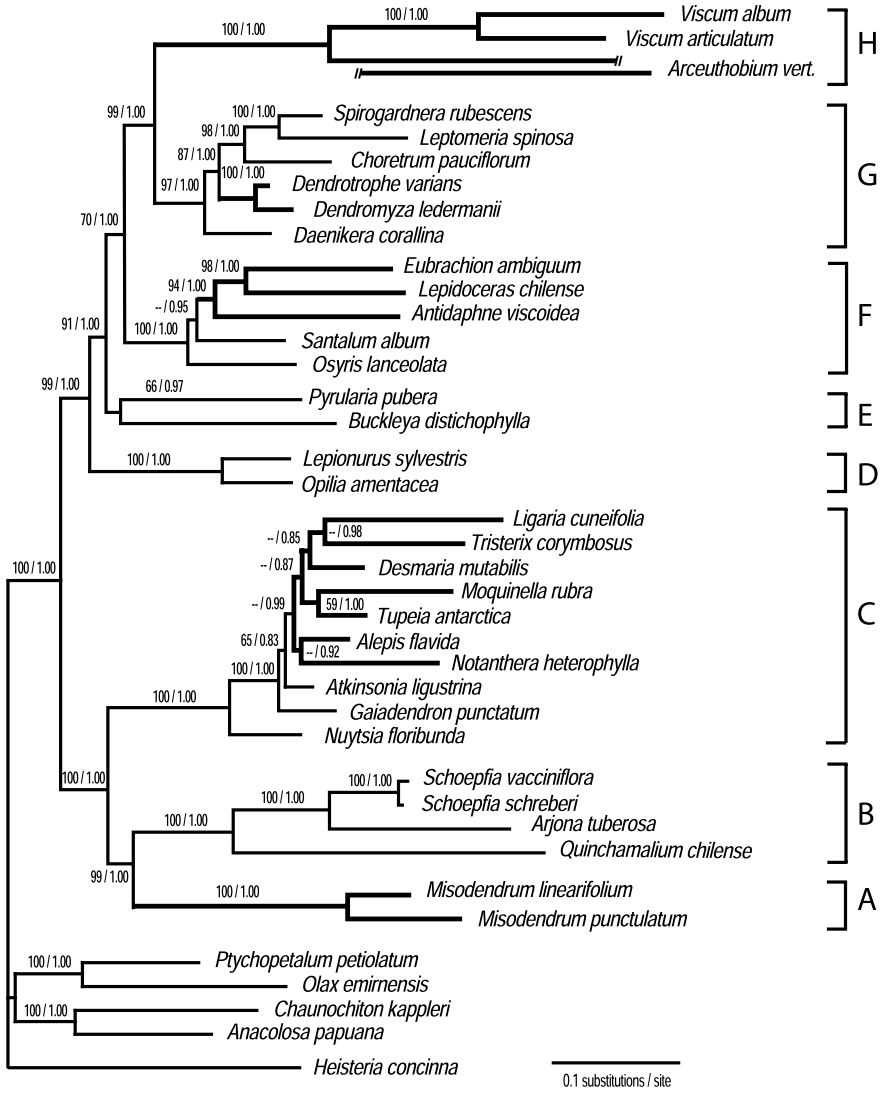

Fig. 2. Majority rule consensus tree from Bayesian analysis of the concatenated five gene dataset. Nodal support is given above the branches as bootstrap values for parsimony and posterior probabilities, respectively. Branch lengths are represented by mean values of the trees resulted from Bayesian analysis. Dark branches represent aerial parasites. Clades discussed in the text are labeled A–H.

3.4. Chronogram from BRMC

The time estimates derived from both the BRMC and PL methods (using one or five crown group calibration points derived from fossils) are shown in Table 2. Except for Loranthaceae, PL gave more recent time estimates than the BRMC. The addition of multiple calibration points did not change the PL estimations but did affect those from the BRMC method. Here the differences between estimates for a taxon derived from the three root node dates were less when multiple calibrations were used. The BRMC estimates with multiple calibrations and the 114 Mya *Saxifraga* root age were used to make the BI tree ultrametric. The resulting chronogram (Fig. 3) shows the relative timing of the evolution of aerial parasitism in Santalales. Among the extant lineages that contain aerial parasites, an absolute age of 80 Mya is obtained for Misodendraceae (clade A) followed by Viscaceae that arose 72 Mya. It should be pointed out that it is not known at which point along the stem of these clades each parasitic lineage acquired the aerial habit. Moreover, relatively large standard deviations are associated with these BRMC estimates, thus whether one or the other family evolved first is statistically equivocal. At 53 Mya, clade F taxa (Eremolepidaceae) evolved next followed by the dendroparasites and mistletoes of Santalaceae tribe Amphorogyneae (46 Mya). Finally, the most recent evolution of aerial parasitism appears to be in Loranthaceae at 28 Mya.

4. Discussion

The present study confirms the previous finding (Nickrent, 2002) that aerial parasitism evolved five times independently in Santalales and, for the first time, assigns dates to these nodes on the phylogenetic tree. Informed by the ultrametric tree reported here, these evolutionary

Table 2
Bayesian relaxed molecular clock (BRMC) with standard deviations and penalized likelihood (PL) time estimates (Mya) for divergence of aerial parasite clades in Santalales given standard errors around a 114 Mya age for the *Saxifraga* root (Wikström et al., 2001)

Clade letter and name	BRMC			PL		
	104	114	124	104	114	124
	Anacolosa calibration point					
A. Misodendraceae	94 (±21)	99 (±23)	103 (±25)	74	81	88
C. Loranthaceae	33 (±09)	34 (±10)	36 (±11)	32	35	38
F. Eremolepidaceae	65 (±16)	68 (±17)	71 (±19)	51	55	60
G. Amphorogyneae	56 (±10)	58 (±16)	61 (±17)	40	44	48
H. Viscaceae	87 (±19)	91 (±22)	94 (±24)	68	75	81
	Anacolosa and four other calibration points					
A. Misodendraceae	79 (±9)	80 (±9)	81 (±9)	74	81	88
C. Loranthaceae	27 (±5)	28 (±6)	28 (±6)	32	35	38
F. Eremolepidaceae	53 (±7)	53 (±7)	54 (±7)	51	55	60
G. Amphorogyneae	46 (±7)	46 (±7)	46 (±8)	40	44	48
H. Viscaceae	71 (±8)	72 (±8)	73 (±8)	68	75	81

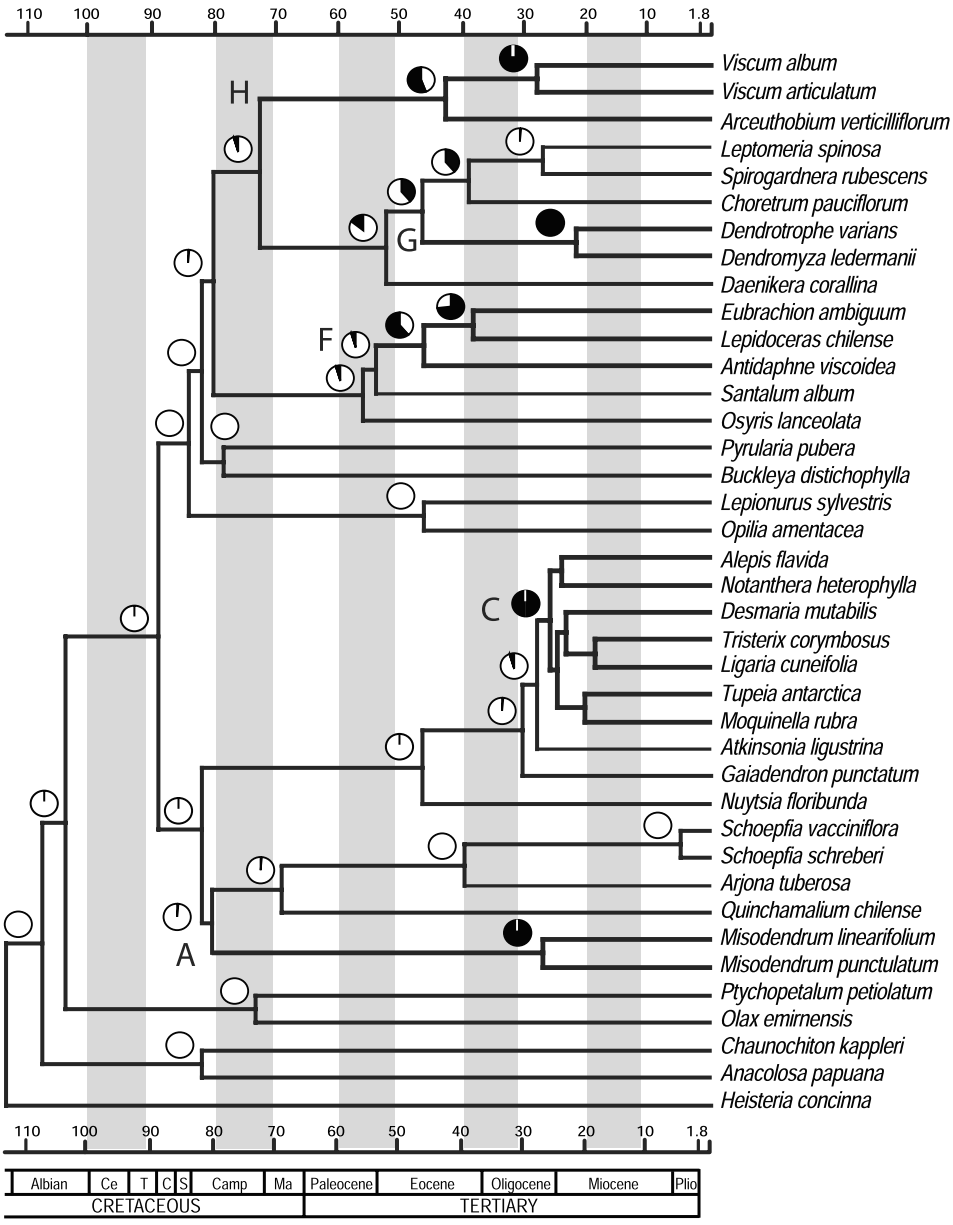

Fig. 3. Chronogram resulting from BRMC analysis. Aerial parasite clades (dark branches) are labeled as in Fig. 1. Pie diagrams derived from Mesquite represent the probabilities of root (white) or aerial (black) parasitism for that node.

events can be better understood by examining various parasitic modes seen throughout Santalales (Fig. 4A–I). In this portion of the Santalales tree the plesiomorphic state is a root parasitic tree or shrub (Fig. 4A), a condition found in the outgroup Olacaceae, as well as three genera of Loranthaceae (*Nuytsia*, *Atkinsonia*, and *Gaiadendron*), Opiliaceae, and some Santalaceae. In root parasitic lianas (Fig. 4B), the aerial shoots clamber and twine through the host tree but no haustoria are formed from aerial parts of the parasite. Examples include *Cansjera* (Opiliaceae) and some Santalaceae (Amphorogyneae), such as *Dendrotrophe varians*. Some mistletoes such as *Tripodanthus acutifolius* (Loranthaceae) initially form primary haustorial connections to host stems and later, by means of adventitious roots, form haustorial connections to host roots (Fig. 4C). These mistletoes may also exist only as aerial parasites. We suggest using the term "*amphiphagous*" to describe a condition where individuals of a species feed upon stems, roots or both simultaneously. The stem parasitic lianas or dendroparasites (Fig. 4D) first attach to host branches by means of a radicular primary haustorium. Through further development, secondary haustoria are produced from roots that arise from the twining stems. Our definition of dendroparasite differs from the one given by Macklin and Parnell (2002) where they equate the term with mistletoe (aerially parasitic non-twining shrubs). In some species of *Dendromyza* (Santalaceae, Amphorogyneae), it appears the shoots are dimorphic in that some are non-twining, foliose, and photosynthetic whereas others are twining, squamate and form haustoria.

Among mistletoes, a number of different haustorial systems (Calvin and Wilson, 2006) can be seen (Fig. 4E–I). Some form a primary haustorial connection to the host and this remains the sole connection throughout the life of the parasite (Fig. 4E). The haustorial endophyte remains localized in the region of original infection. Examples of this include *Misodendrum*, many Loranthaceae (e.g., *Englerina*, *Lysiana*, *Psittacanthus*, *Tapinanthus*), *Dufrenoya* (Amphorogyneae), and some Viscaceae. In other mistletoes, a primary haustorium is formed but the endophyte (bark strand) spreads laterally within the host cortex distal to the point of original infection (Fig. 4F). Examples of this type in Loranthaceae include *Diplatia*, *Moquiniella*, *Tristerix* and *Tupeia*. A variation also occurs where the bark strands are capable of initiating secondary shoots (Fig. 4G) such as in *Agelanthus*, *Oncocalyx*, and *Helixanthera* (all Loranthaceae). Some mistletoes are capable of forming epicortical roots that "explore" the host surface and form secondary haustorial connections (Calvin and Wilson, 2006). Fig. 4H is meant to represent all variants of this type in that some epicortical roots arise from haustoria and some from shoots. Shoots frequently occur at the site where secondary haustorial connections are made. Examples include many Loranthaceae such as *Alepis*, *Desmaria*, *Notanthera*, and *Scurrula*. The squamate mistletoes (Fig. 4I) are here recognized as different from the type shown in Fig. 4G only to emphasize the presence of scale leaves with lowered photosynthetic activity. This type is seen in *Misodendrum*, *Phacellaria* and *Arceuthobium*.

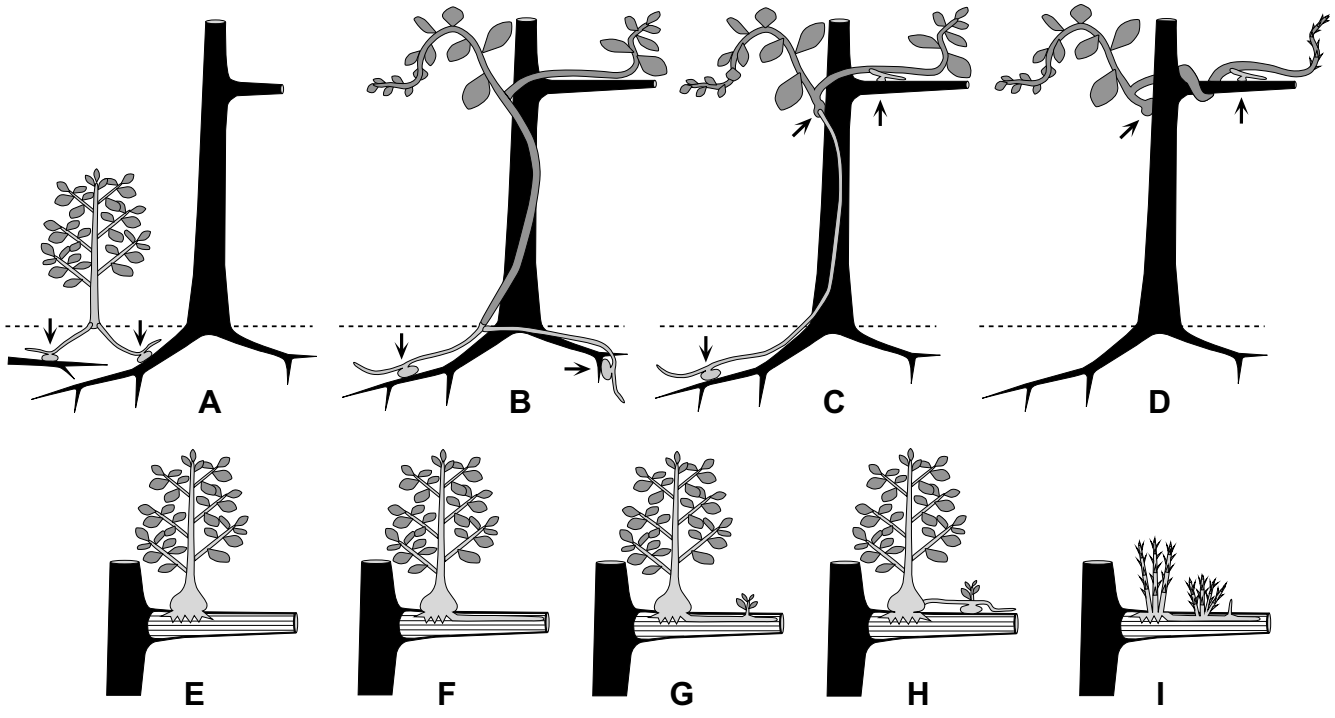

Fig. 4. Parasitic modes present in Santalales. Arrows for A–D represent haustorial connection points. See text for explanation.

4.1. The Misodendraceae clade

Given the standard deviations associated with the dates of divergence for Viscaceae and Misodendraceae, it cannot be unambiguously determined which lineage first evolved aerial parasitism. We propose, however, that Misodendraceae most likely represent the first mistletoes because the divergence date of 80 Mya is older than that obtained for Viscaceae (72 Mya). Moreover, the Mesquite analysis gave an 0.6 probability that the ancestor of Viscaceae was aerial whereas for Misodendraceae the probability was near 1.0 (Fig. 3). Although fossil pollen for *Misodendrum* (as *Compositoipollenites*) are not known from strata older than Oligocene, this is a minimum age and older fossils likely exist but remain undiscovered. Furthermore, we suggest that divergence times for Viscaceae on the chronogram (Fig. 3) have been artifactually inflated owing to among lineage rate heterogeneity (see below). The difference between the stem and crown group ages for the Misodendraceae clade spans 53 million years. As no macrofossils are available and only nodal dates are estimated, we cannot determine at which point along this long-branch aerial parasitism appeared. Because Misodendraceae are a small and apparently old family (Vidal-Russell and Nickrent, 2007), and that past extinctions have gone unrecognized, the timing of diversification may be underestimated. The phylogenetic history of *Misodendrum* must be closely tied to that of its only host, *Nothofagus* (southern beech). The fossil record for *Nothofagus* suggests a Cretaceous origin for the genus in the early Campanian and all subgenera were differentiated by 75 Mya (Dettmann et al., 1990; Knapp et al., 2005). The time estimate from molecular data for the divergence of Nothofagaceae from the remaining Fagales was 93 Mya (Cook and Crisp, 2005). Given the coincidental timing of the origin of *Nothofagus* and *Misodendrum*, it is possible that these two taxa codiversified during the Cretaceous.

The Misodendraceae clade is sister to one containing *Schoepfia*, *Arjona* and *Quinchamalium*. *Schoepfia* has most frequently resided in Olacaceae, but its position on molecular phylogenetic trees supports its classification in a separate family, Schoepfiaceae (Nickrent et al., 1998; Nickrent and Malécot, 2001). These results support those of Der and Nickrent (2008) who also included the South American root parasites *Arjona* and *Quinchamalium* in Schoepfiaceae, not Santalaceae.

4.2. The Loranthaceae clade

As reviewed in Section 1, pollen associated with Loranthaceae (loranths) has been described from numerous locations in strata dated to Late Cretaceous. This correlates well with the divergence date for the loranth clade reported here as 81 Mya (Fig. 3). Because the three root parasitic genera in the family (*Nuytsia*, *Gaiadendron*, and *Atkinsonia*) are successive sister taxa to all aerial parasites, it is most parsimonious to envision the ancestral loranth as a root parasite, not an aerially parasitic mistletoe. If the ancestral loranth was a stem parasite, the tree topology requires three reversions to root parasitism. We consider this scenario less likely based simply on parsimony (but see below). The ancestral root parasitic loranth likely existed in warm tropical to subtropical conditions and may have been arborescent. This follows from the habit of *Nuytsia* which speciated first from the main loranth lineage during the Eocene. Our analyses indicate that the acquisition of aerial parasitism in Loranthaceae occurred once and was probably a more recent event than any of the other four mistletoe lineages (28 Mya). Branch lengths between aerially parasitic loranth genera are very short, suggesting a rapid diversification during the Oligocene. This epoch marked the start of global cooling where tropical regions diminished giving way to temperate deciduous woodlands and grasslands. Today, savanna biomes of Africa and Australia support an extremely rich loranth flora, thus suggesting this habitat type provided the environment favoring the rapid diversification of these mistletoes.

Are there recorded cases of aerially parasitic loranths "reverting" to root parasitism? Most species of the genus *Helixanthera*, a genus that ranges from Africa to Indomalaya, are stem parasites. The Chinese species *Helixanthera terrestris* and *H. scoriarum* are cited as being terrestrial root parasites (Huaxing et al., 2003), thus suggesting evolutionary reversions or atavism. These observations need to be confirmed because parasitism of small shrubs, especially ones with atrophied branches, can be misleading. In the case of *Tripodanthus acutifolius* (Fig. 4C), it appears that the mistletoe is first established on host branches and then attaches to roots via secondary haustoria derived from adventitious roots (Kuijt, 1982). With regard to *Gaiadendron*, Kuijt (1963) observed terrestrial as well as epiphytic individuals, but makes the point that the distinction between these zones is not always meaningful. It is possible that *Gaiadendron* starts as a seedling in the soil, attaches to roots (or rhizomes) and grows upward into the host tree where it then forms secondary haustorial connections. Alternately, its seeds could lodge in crevices between host branches where humus has accumulated. Following germination, the seedling could attach to roots of the surrounding epiphytes or to young host branches.

4.3. The "Eremolepidaceae" clade

Fossil pollen of *Antidaphne* is known from the mid Eocene of Chile (Darrah, 1939 and references therein). This date is ca. 5 Mya more recent than the molecular estimation for the divergence time of this genus from the *Lepidoceras* and *Eubrachion* clade. Although only two root parasites were used to represent this clade (*Santalum* and *Osyris*), a complete molecular phylogeny of Santalaceae (Der and Nickrent, 2008) added *Colpoon*, *Rhoiacarpos*, *Nestronia*, *Mysoschilos*, and *Exocarpos*, the latter sister to the entire clade. Among the 26 species of the genus *Exocarpos*, at least two have been reported to parasitize either

roots or stems (Lam, 1945; Kuijt, 1969). This, in conjunction with a 0.6 probability that the ancestor of the eremolepidaceous parasites was an aerial parasite (Fig. 3), suggests that the amphiphagous habit provided the genetic preadaptation for the evolution of stem parasitism in these mistletoes.

4.4. The Santalaceae—Amphorogyneae clade

Among the paraphyletic Santalaceae, the second lineage to evolve aerial parasitism are various members of tribe Amphorogyneae. This remarkable group of plants, first taxonomically recognized by Stauffer (1969), includes what might be considered a transition series of parasitic habits—root parasites (*Choretrum* and *Leptomeria*), amphiphagous parasites (*Daenikera* and possibly *Dendrotrophe)*, dendroparasites (*Dendromyza*), mistletoes (*Dufrenoya*) and hyperparasitic mistletoes (*Phacellaria*). *Daenikera corallina* is typically seen as a root parasite, but some individuals emerge at the base or even some distance up the stem of the host tree. It has been suggested that this taxon is a holoparasite, but as noted by Hürlimann and Stauffer (1957), there is chlorophyll in the epidermis but it is masked by red pigments. Moreover, we report here an *rbcL* sequence for *Daenikera* that is full-length, does not show an increased substitution rate relative to other Amphorogyneae, and has no amino acid replacements that might suggest lack of functionality. Therefore, this plant may be compared to other flabellate, red-pigmented, photosynthetic Santalaceae such as *Exocarpos casuarinoides*.

The chronogram (Fig. 3) shows that the aerial parasites of tribe Amphorogyneae (*Dendrophthoe* and *Dendromyza*) evolved at the beginning of the Eocene. No conclusive fossils exists for any member of this tribe, possibly because the entemophilous members produce low amounts of pollen and because the Australian root parasites occur in dry areas. Moreover, pollen from extant genera present few distinguishing features that would allow identification of existing palynomorphs. Older references to *Leptomeria* from Baltic amber (Pilger, 1935) are likely not equivalent to the modern genus that is endemic to Australia.

Because Amphorogyneae is sister to Viscaceae (all of which are stem parasitic mistletoes) their common ancestor could be envisioned as an aerial parasite. But because *Daenikera* is sister to the Amphorogyneae clade, and it is amphiphagous, it seems reasonable to propose this parasitic mode for the ancestor. In fact the probability that this ancestor was aerial is only 0.10, increasing to 0.6 in the lineage leading to Viscaceae (Fig. 3). Specialization in Viscaceae was entirely toward the mistletoe habit whereas in Amphorogyneae, this polymorphism was maintained in the basal lineages. Mistletoes such as *Dufrenoya* and *Phacellaria* thus evolved independently from Viscaceae. The genera *Choretrum, Leptomeria*, and *Spirogardnera* are all root parasites, thus suggesting they lost (or do not express) the ability to parasitize stems, or they descended from individuals that were already root parasites. This may be correlated with their increased ability, as compared with stem parasites, to survive fire via regeneration from underground parts, as these plants grow in fire-prone areas.

4.5. The Viscaceae clade

Viscaceae apparently diverged early (72 Mya) from the common ancestor it shared with Amphorogyneae. As discussed above, this date competes with the one for Misodendraceae as the oldest lineage of aerial parasite, but we consider the date inflated owing to rate heterogeneity. Within Santalales, rate acceleration was first observed for Viscaceae, particularly *Arceuthobium* (Nickrent and Franchina, 1990; Nickrent and Starr, 1994). Viscaceae show longer branches than the rest of the taxa (Fig. 1) and rate increases are affecting both nuclear and chloroplast genomes, in agreement with Nickrent et al. (1998).

All Viscaceae are mistletoes that form primary haustorial connections but do not produce epicortical roots (as in some Loranthaceae). Lateral spread of the endophyte within the host cortex does occur and new shoots may arise at positions distal to the original infection (Fig. 4G). The most elaborate manifestation of endophytic growth is the production of systemic (isophasic) "witches' brooms" in some species of *Arceuthobium* where the parasite endophyte grows in synchrony with the host apical meristem.

4.6. Evolution of the mistletoe habit

The data presented here can now be generalized to help address questions relating to the evolution of the mistletoe habit. All five mistletoe clades appear to have evolved from root parasitic ancestors. In four of these clades there is evidence for preadaptation to stem parasitism in amphiphagous taxa (and also assumed present in ancestral nodes). These are *Gaiadendron* (Loranthaceae), *Exocarpos* (eremolepidaceous clade), *Daenikera* (Amphorogyneae), and the common ancestor of the latter and Viscaceae. The evolutionary directionality of this character state change is strongly biased from root to stem parasitism. Cases of potential reversion to root parasitism, such as in *Helixanthera* and *Tripodanthus* (Loranthaceae), possibly indicate atavism. That such events are rare suggest that aerial parasitism is a successful trophic mode under strong positive selection. The Misodendraceae clade is sister to a clade with only root parasites (*Schoepfia, Arjona* and *Quinchamalium*), thus the *Misodendrum* ancestor presumably was root parasitic. Given the evolutionary transitions seen in other mistletoe lineages, it is conceivable that the ancestor of *Misodendrum* also passed through an amphiphagous condition prior to becoming an aerial parasite.

Misodendraceae and Viscaceae were apparently the first lineages to evolve stem parasitism. They also have a high degree of specialization in morphological features. Thus, we hypothesize that during this long evolutionary time period positive selection for some traits and relaxation of selection in others resulted in their highly derived condi-

tions. In Loranthaceae, whose diversification occurred more recently and rapidly (see shorter branches in Fig. 2), such profound changes are not seen. Most genera in Loranthaceae show a higher number of plesiomorphic characters, e.g., epicortical roots. These are also present in some members of the eremolepidaceous lineage, but are absent in Viscaceae and Misodendraceae that developed cortical strands through endophytic growth (Fig. 4F and G). Such cortical strand growth is seen in only ten of the 73 genera of Loranthaceae.

Mistletoe evolution provides good examples of convergence in several morphological traits. Leaves reduced to scales (the squamate condition) as seen in *Arceuthobium* (Viscaceae) are strikingly similar to those in *Misodendrum*. These squamate mistletoes are also characterized by reduction in chlorophyll content and small, unisexual flowers. This suite of features is present in *Eubrachion* of the eremolepidaceous lineage and *Phacellaria* and *Daenikera* of Amphorogyneae. Curiously, the squamate habit has rarely evolved among the 900 species of Loranthaceae. Although many genera show a high degree of floral reduction, *Ixocactus hutchisonii* represents the only example of a squamate loranth whose phylloclades (not leaves) are photosynthetic (Kuijt, 1967). Paucity of this growth form may mean that this trait is associated with a trend towards holoparasitism, which is essentially absent in Loranthaceae. Among the five mistletoe lineages, different evolutionary "experiments" have taken place that resulted in attachment structures on the seeds or fruits. In *Misodendrum* the achenes bear long, plumose staminodes that first keep the fruit aloft and then serve to anchor it onto the host branch. Viscin coated seeds are seen in Loranthaceae, Viscaceae, the eremolepidaceous clade, and some members of Amphorogyneae (*Dufrenoya* and *Phacellaria*) but these attachment structures have different developmental origins and are thus not homologous.

The phylogenetic tree presented in Fig. 2 has two major clades that suggest southern (clades A–C) and northern (clades D–H) hemisphere origins for these families. Loranthaceae are usually cited as having arisen on Gondwana whereas Viscaceae evolved on the Laurasian landmass (Barlow, 1983). As discussed above, it appears Loranthaceae underwent a major radiation during the Oligocene, but this was preceded by a massive dispersal throughout Gondwana as early as the Cretaceous (Barlow, 1983). Santalaceae and Viscaceae do not have relictual occurrences on southern landmasses and thus are likely of northern origin. Essentially nothing has been written about the biogeographic history of Santalaceae, thus most interpretations must derive from the fossil record and the distributions and molecular phylogenies of extant taxa. Phylogenetic evidence (Der and Nickrent, 2008) indicates the entirely New World eremolepidaceous taxa diverged early in the clade, possibly from a root parasite similar to extant *Myoschilos*. The sister to all other members of the Amphorogyneae clade, *Daenikera*, is a New Caledonian endemic whereas the root parasites are found in Australia and the dendroparasites and mistletoes range from Queensland through Indomalaya to China and southern Asia. Based on morphological features Stauffer and Hurlimann (1957) considered *Amphorogyne* and *Daenikera* as primitive and relictual, a position supported by the molecular phylogenetic topology presented here. This suggests a southern origin for Amphorogyneae, not northern as seen in Viscaceae and other clades of "Santalaceae".

4.7. Reliability of the chronogram and fossil data

Error associated with the dates assigned to the various nodes on the chronogram derives mainly from two sources: (1) the robustness of the molecular phylogeny and (2) the age and identity of the fossil pollen used for calibrating the tree. With regard to topology, our multigene tree for Santalales has higher support for the nodes along the "spine" (i.e., interfamilial relationships) than any previously published one. However, even when the topology of the tree is reliable, rate heterogeneity will artifactually inflate divergence times. In our case, the longest branches on the tree were associated with Viscaceae. Although the r8s program constrains the rate of change from ancestral to derived lineages, simulations have shown that it is difficult to estimate divergence times with heterogeneous rates (Sanderson, 1997). Despite this, divergence times estimates from BRMC and PL in Santalales were comparable, as was observed in a broader study of all angiosperms (Bell et al., 2005).

The second limitation relates to the microfossil data. It is difficult to precisely place a fossil taxon with the stem or crown group because a phylogenetic (cladistic) analysis must be conducted that simultaneously includes fossil and extant taxa, after which diagnostic synapomorphies must be identified. As pointed out by Magallon and Sanderson (2001) this has rarely been done with angiosperms. Pollen represents the vast majority of fossils available for Santalales, thus these must be used in comparisons with extant genera to determine affinities. In contrast to Loranthaceae, pollen from essentially all of the genera of Santalaceae have been described (Feuer, 1977; Feuer and Kuijt, 1978; Kuijt, 1988). Despite this, to date no formal cladistic analysis of these data has been conducted that would allow integration of the fossil pollen data. Such studies would help determine whether the fossil pollen is: (1) congeneric with a crown group member, (2) an extinct member of the crown group, (3) an extinct stem group representative that is sister to the crown group, or (4) a member of a clade sister to the stem group. As with all morphological data, patterns of variation in pollen are complex and compromised by intrageneric polymorphism and convergence. Additional comprehensive studies, such as the one conducted by Malécot and Lobreau-Callen (2005) on *Anacolosidites*, are required to sort out which pollen types are most likely related to extant santalalean families and genera.

Acknowledgments

The authors thank the numerous collectors listed in Table 1 who helped obtain specimens for this project, Missouri Botanical Garden for allowing a portion of the *Schoepfia fragrans* sample to be used for DNA extraction, J. Der and V. Malécot for use of unpublished DNA sequences, and S. Sipes for generously allowing use of her automated DNA sequencer. Comments from two anonymous reviewers were helpful in improving this manuscript. Financial support (to R.V.R.) was provided by a Ph.D. fellowship from the Fulbright Commission Argentina, SIUC Graduate School and grants from the National Science Foundation (to D.L.N.).

References

APG, 1998. An ordinal classification for the families of flowering plants. Ann. Mo. Bot. Gard. 85, 531–553.

APG, 2003. An update of the Angiosperm Phylogeny Group classification for the orders and families of flowering plants: APG II. Bot. J. Linn. Soc. Lond. 141, 399–436.

Barlow, B.A., 1964. Classification of the Loranthaceae and Viscaceae. Proc. Linn. Soc. N. S. W. 89, 268–272.

Barlow, B.A., 1983. Biogeography of Loranthaceae and Viscaceae. In: Calder, D.M., Bernhardt, P. (Eds.), The Biology of Mistletoes. Academic Press, New York, pp. 19–45.

Bell, C.D., Soltis, D.E., Soltis, P.S., 2005. The age of the angiosperms: a molecular timescale without a clock. Evolution 59, 1245–1258.

Bhatnagar, S.P., Johri, B.M., 1983. Embryology of Loranthaceae. In: Calder, D.M., Bernhardt, P. (Eds.), The Biology of Mistletoes. Academic Press, New York, pp. 47–66.

Calvin, C.L., Wilson, A.C., 2006. Comparative morphology of epicortical roots in Old and New World Loranthaceae with reference to root types, origin, patterns of longitudinal extension, and potential for clonal growth. Flora 201, 51–64.

Chlonova, A.F., 1962. Some morphological types of spores and pollen grain from Upper Cretaceous of the eastern part of the west Siberian lowland. Pollen Spores, 298–309.

Christopher, R.A., 1979. Normapolles and triporate pollen assemblages from the Raritan and Magothy formations (Upper Cretaceous) of New Jersey. Palynology 3, 73–121.

Cook, L.G., Crisp, M.D., 2005. Not so ancient: the extant crown group of *Nothofagus* represents a post-Gondwanan radiation. Proc. R. Soc. B 272, 2535–2544.

Couper, R.A., 1960. New Zealand Mesozoic and Cenozoic plant microfossils. N. Z. Geol. Surv., Palaeontol. Bull. 32, 1–87.

Darrah, W.C., 1939. Textbook of Paleobotany. D. Appleton-Century, New York.

Der, J.P., Nickrent, D.L., 2008. A molecular phylogeny of Santalaceae (Santalales). Syst. Bot. 33, 107–116.

Dettmann, M.E., Pocknall, D.T., Romero, E.J., Zamaloa, M.C., 1990. *Nothofagidites* Erdtman ex Potonie, 1960: a catalogue of species with notes on the paleogeographic distribution of *Nothofagus* Bl. (Southern Beech). New Zealand Geological Survey, Lower Hutt, New Zealand.

Elsik, W.C., 1974. Characteristic Eocene palynomorphs in the Gulf Coast, U.S.A. Palaeontographica B 149, 90–111.

Feuer, S.M., 1977. Pollen Morphology and Evolution in the Santalales s. str., a Parasitic Order of Flowering Plants. University of Massachusetts, Amherst, p. 426.

Feuer, S., Kuijt, J., 1978. Fine structure of mistletoe pollen I. Eremolepidaceae, *Lepidoceras*, and *Tupeia*. Can. J. Bot. 56, 2853–2864.

Feuer, S., Kuijt, J., 1979. Fine structure of mistletoe pollen II. Pollen evolution in the genus *Psittacanthus*. Mart. Bot. Not. 132, 295–309.

Feuer, S., Kuijt, J., 1980. Fine structure of mistletoe pollen. III. Large-flowered neotropical Loranthaceae and their Australian relatives. Am. J. Bot. 67, 34–50.

Feuer, S., Kuijt, J., 1985. Fine structure of mistletoe pollen. VI. Small flowered neotropical Loranthaceae. Ann. Mo. Bot. Gard. 72, 187–212.

Han, R.-L., Zhang, D.-X., Hao, G., 2004. Pollen morphology of the Loranthaceae from China. Acta Phytotaxonomica Sin. 42, 436–456.

Huaxing, Q., Hua-hsing, C., Hua-xing, K., Gilbert, M.G., 2003. Loranthaceae. Flora China 5, 220–239.

Huelsenbeck, J., Ronquist, F., 2001. MrBayes. Bayesian inference of phylogeny. Bioinformatics 17, 754–755.

Huelsenbeck, J.P., Larget, B., Swofford, D., 2000. A compound Poisson process for relaxing the molecular clock. Genetics 154, 1879–1892.

Hürlimann, H., Stauffer, H.U., 1957. Santalales-Studien II. Daenikera, eine neue Santalaceen-Gattung. Vierteljahrsschrift Naturf. Ges. Zürich 102, 332–336.

Jarzen, D.M., 1977. *Aquilapollenites* and some santalalean genera; a botanical comparison. Grana 16, 29–39.

Jarzen, D.M., 1978. The terrestrial palynoflora from the Cretaceous-Tertiary transition, Alabama, U.S.A. Pollen Spores 20, 535–553.

Knapp, M., Stöckler, K., Havell, D., Delsuc, F., Sebastiani, F., Lockhart, P.J., 2005. Relaxed molecular clock provides evidence for long-distance dispersal of *Nothofagus* (Southern Beech). PLoS Biol. 3, e14.

Krutzsch, W., 1962. Stratigraphisch bzw. botanisch wichtige neue Sporen und Pollen formen aus dem deutschen Tertiar. Geologie 11, 265–319.

Kuijt, J., 1963. On the ecology and parasitism of the Costa Rican tree mistletoe, *Gaiadendron punctatum* (Ruiz and Pavón) G. Don. Can. J. Bot. 41, 927–938.

Kuijt, J., 1967. The genus *Ixocactus* (Loranthaceae, s.s.): description of its first species. Brittonia 19, 61–66.

Kuijt, J., 1968. Mutual affinities of santalalean families. Brittonia 20, 136–147.

Kuijt, J., 1969. The Biology of Parasitic Flowering Plants. University of California Press, Berkeley, CA.

Kuijt, J., 1982. Epicortical roots and vegetative reproduction in Loranthaceae (s.s.) of the New World. Beitr. Biol. Pflanzen 56, 307–316.

Kuijt, J., 1988. Monograph of Eremolepidaceae. Syst. Bot. Monogr. 18, 1–60.

Lam, H.J., 1945. Fragmenta Papuana. Sargentia 5, 1–196.

Macklin, J., Parnell, J., 2002. An account of the Santalaceae of Thailand. Thai. For. Bull. 30, 75–115.

Macphail, M., Cantrill, D.J., 2006. Age and implications of the Forest Bed, Falkland Islands, southwest Atlantic Ocean: evidence from fossil pollen and spores. Palaeogeogr. Palaeoclimatol. Palaeoecol. 240, 602–629.

Maddison, W.P., Maddison, D.R., 2006. Mesquite: a modular system for evolutionary analysis. Version 1.12. Available from: http://mesquiteproject.org.

Magallon, S., Sanderson, M., 2001. Absolute diversification rates in angiosperm clades. Evolution 55, 1762–1780.

Malécot, V., Lobreau-Callen, D., 2005. A survey of species assigned to the fossil pollen genus *Anacolosidites*. Grana 44, 314–336.

Martin, H.A., 1982. Changing Cenozoic barriers and the Australian Paleobotanical record. Ann. Mo. Bot. Gard. 69, 625–667.

Menke, B., 1976. Pliozane und altestquartare Sporen und Pollenflora von Schleswigholstein. Geol. Jahrb. A 32, 3–197.

Mildenhall, D.C., 1980. New Zealand Late Cretaceous and Cenozoic plant biogeography: a contribution. Palaeogeogr. Palaeoclimatol. Palaeoecol. 31, 197–233.

Muller, J., 1981. Fossil pollen records of extant angiosperms. Bot. Rev. 47, 1–142.

Muller, J., 1984. Significance of fossil pollen for angiosperm history. Ann. Mo. Bot. Gard. 71, 419–443.

Nickrent, D.L., 1994. From field to film: rapid sequencing methods for field collected plant species. BioTechniques 16, 470–475.

Nickrent, D.L., 1997. The Parasitic Plant Connection. Southern Illinois University, Carbondale, USA. Available from: http://www.parasitic-plants.siu.edu/.

Nickrent, D.L., 2002. Mistletoe phylogenetics: current relationships gained from analysis of DNA sequences. In: Angwin, P. (Ed.), Proceedings of the Forty-eighth Western International Forest Disease Work Conference. USDA Forest Service, Redding, California, Kona, Hawai'i, pp. 48–57.

Nickrent, D.L., Duff, R.J., Colwell, A.E., Wolfe, A.D., Young, N.D., Steiner, K.E., dePamphilis, C.W., 1998. Molecular phylogenetic and evolutionary studies of parasitic plants. In: Soltis, D.E., Soltis, P.S., Doyle, J.J. (Eds.), Molecular Systematics of Plants II. DNA Sequencing. Kluwer Academic Publishers, Boston, MA, pp. 211–241.

Nickrent, D.L., Franchina, C.R., 1990. Phylogenetic relationships of the Santalales and relatives. J. Mol. Evol. 31, 294–301.

Nickrent, D.L., Malécot, V., 2001. A molecular phylogeny of Santalales. In: Fer, A., Thalouarn, P., Joel, D.M., Musselman, L.J., Parker, C., Verkleij, J.A.C. (Eds.), Proceedings of the 7th International Parasitic Weed Symposium. Faculté des Sciences, Université de Nantes, Nantes, France, pp. 69–74.

Nickrent, D.L., Starr, E.M., 1994. High rates of nucleotide substitution in nuclear small-subunit (18S) rDNA from holoparasitic flowering plants. J. Mol. Evol. 39, 62–70.

Nylander, J.A., 2004. MrModelTest. Distributed by the author. Evolutionary Biology Centre, Uppsala University, Upsalla.

Pilger, R., 1935. Santalaceae. In: Engler, A., Prantl, K. (Eds.), Die Natürlichen Pflanzen Familien. Wilhelm Engelman, Leipzig, pp. 52–91.

Rambaut, A., 2004. Se–Al Sequence Alignment Editor. Department of Zoology, University of Oxford, Oxford, UK.

Ronquist, F., Huelsenbeck, J., 2003. MrBayes 3: Bayesian phylogenetic inference under mixed models. Bioinformatics 19, 1572–1574.

Rutschmann, F., 2005. Bayesian Molecular Dating Using PAML/multidivtime. A Step-by-Step Manual. University of Zurich, Zurich.

Sanderson, M., 1997. A nonparametric approach to estimating divergence times in the absence of rate constancy. Mol. Biol. Evol. 14, 1218–1231.

Sanderson, M., 2002. Estimating absolute rates of molecular evolution and divergence times: a penalized likelihood approach. Mol. Biol. Evol. 19, 101–109.

Sanderson, M.J., 2003. r8s: inferring absolute rates of molecular evolution and divergence times in the absence of a molecular clock. Bioinformatics 19, 301–302.

Selmeier, A., 1975. *Viscoxylon pini* Novum Genus et Nova Species, Mistel-Senker in einem verkieselten *Pinus*-Holz aus jungtertiaren Sedimenten von Falkenberg, Oberpfalz (Bayern). Ber. Bayer Bot. Ges. Erforsch Heim. Flora 46, 93–109.

Soltis, D.E., Soltis, P.S., Endress, P.K., Chase, M.W., 2005. Phylogeny and Evolution of Angiosperms. Sinauer Associates, Inc., Sunderland, MA.

Stauffer, H.U., 1969. Santalales Studien X. Amphorogyneae eine neue Tribus der Santalaceae. Vierteljahrsschr. Naturf. Ges. Zürich 114, 49–76.

Stauffer, H.U., Hurlimann, H., 1957. Santalales-Studien III. *Amphorogyne*, eine weitere Santalaceen-Gattung aus Neukaledonien. Vierteljahrsschr. Naturf. Ges. Zürich 102, 337–349.

Stearn, W.T., 1972. *Kunkeliella*, a new genus of Santalaceae in the Canary Islands. Cuad. Bot. Canar. 16, 11–26.

Swofford, D.L., 2003. PAUP*: Phylogenetic Analysis Using Parsimony (* and Other Methods). Sinauer Associates, Sunderland, MA.

Taberlet, P., Gielly, L., Pautou, G., Bouvet, J., 1991. Universal primers for amplification of three non-coding regions of chloroplast DNA. Plant Mol. Biol. 17, 1105–1109.

Taylor, D.W., 1989. Select palynomorphs from the Middle Eocene Claiborne Formation, Tenn. (U.S.A.). Rev. Paleobot. Palynol. 58, 111–128.

Thorne, J.L., Kishino, H., Painter, I.S., 1998. Estimating the rate of evolution of the rate of molecular evolution. Mol. Biol. Evol. 15, 1647–1657.

Vidal-Russell, R., Nickrent, D.L., 2007. A molecular phylogeny of the feathery mistletoe *Misodendrum*. Systematic Botany 32, 560–568.

Wiens, D., Barlow, B.A., 1971. The cytogeography and relationships of the viscaceous and eremolepidaceous mistletoes. Taxon 20, 313–332.

Wikström, N., Savolainen, V., Chase, M., 2001. Evolution of the angiosperms: calibrating the family tree. Proc. R. Soc. Lond. B Biol. Sci. 268, 2211–2220.

Yang, Z., 1997. PAML: a program package for phylogenetic analysis by maximum likelihood. Comput. Appl. Biosci. 13, 555–556.